Catalyst deactivation by aromatics during LCO upgrading to high quality diesel
Proceedings of European Congress of Chemical Engineering (ECCE-6)
Copenhagen, 16-20 September 2007

Catalyst deactivation during LCO upgrade to high-quality diesel

Roberto Galiasso Tailleur[1]

Department of Chemical Engineering, Texas A&M University, College Station, Texas

Abstract

Diesel fuels of 50 and 15 ppm of sulfur content were produced in a pilot plant by upgrading light catalytic cracking gas oil (LCO) during 10 weeks of continuous operation. The end-of-run catalysts were characterized before and after soluble coke extraction by CH_2Cl_2. The cokes were characterized by ^{13}CNMR, TPO, GC-MS, and elemental analysis. Catalyst surfaces were characterized by XPS, CO adsorption, pyridine adsorption, and chemical reactions. The results indicate important differences in amount and composition of the soluble type of coke on the two deactivated catalysts. Soluble coke differently affected the accessibility to the catalyst actives sites in both samples. Catalyst deactivation is higher and ring opening reaction rate lower with greater hydrotreating severity used to achieve 5 ppm instead of 50 ppm of sulfur.

Keyword: LCO upgrading, low aromatic diesel, catalyst deactivation, $WNiPd/TiO_2Al_2O_3$

1. Introduction

A considerable number of recent papers examine the benefits of the new HDS catalyst and potential modifications in the units used in processing that will serve to achieve the 15 ppm target [1-4]. On the other hand, limited attention has been devoted to solving the aromatics problem with new catalyst design and determining how much cracked diesel components should be incorporated into the pool. The newest generation of HDS catalysts achieves more than three times better activity than those of the previous generation. Still, with the new-generation catalysts, about twice the amount of active catalyst is required to reduce density and polyaromatics content and to improve cetane number for premium diesel fuel production. The key issue in polyaromatic hydrogenation is the ring-opening reaction that allows improvement of the cetane number and reduces thermodynamic equilibrium that may control hydrogenation reaction rates. The upgrading of light catalytic cracking oil (LCO) and straight run (SRGO) gas oil fractions to produce a low-sulfur high cetane number diesel is a growing area of interest. The chemistry and associated catalysis for deep desulfurization and deep dearomatization (hydrogenation) was recently reviewed by Song and Ma, 2006 [5], who noticed the inhibiting effect of polyaromatics and nitrogen compounds on sulfur removal when a product with 15 ppm sulfur content is needed. The addition of LCO to the straight-run gas oil increases the aromatic content and produces an important reduction in the apparent rate of reactions [4]. The effect of LCO on activity, selectivity, and stability is discussed in reference [4], among others.

In hydroprocessing of petroleum products, catalyst deactivation by coke deposition is one of the major concerns of the petroleum and petrochemical industries, both from the economic and technological points of view [6–10]. Coke deposition occurs in the pores and/or on the surface of the catalysts, and always leads to loss of activity and product selectivity. Thus,

[1] Corresponding author: Texas A&M University, Department of Chemical Engineering, College Station, Texas 77843-3122, Tel. 1 979-218-1903, galiassa@cantv.net

the first remedy of deactivation has always been linked to the development of coking-resistant catalysts. To obtain necessary information for process design and optimization of these types of catalysts, a great deal of effort has been devoted to studying the chemistry of coke formation with emphasis on the nature and composition of coke. However, there is still a lack of detailed mechanistic knowledge of coke formation, due largely to problems associated with the comprehensive structural characterization of the insoluble organic matter present in relatively low concentrations. A significant improvement in understanding was achieved by new analytical techniques used for coke characterization (for example, Song and Ma [5], among others). In spite of these advances, the effect of coke on active phase for hydrotreating catalyst is not well understood due to the complex nature of the active sites and the coke itself.

During commercial operation of the hydrotreating units that process LCO, relative changes in the hydrogenation, hydrogenolysis, isomerization, and cracking reactions as a function of time on stream [11] were observed. The temperature was increased along the cycle to maintain a constant level of sulfur in the product. Both the metal and acid sites were deactivated at different rates, but deactivation of the acid site function had more impact on product quality than acid sites. The deactivation of the latter sites are responsible for the naphthenic ring opening, paraffin cracking, and dealkylation reactions that produced an increase in aromatics content and a reduction in cetane number as a function of time on stream. This behavior was confirmed in the pilot plant test where pure LCO was tested in a three-month cycle using a WNiPd/TiO_2 Al_2O_3 catalyst [12].

The present work focuses on understanding the effect of hydrotreating severity during upgrade of LCO into an ultra-low-sulfur diesel, on coke deposition, as well as in activity and selectivity in converting polyaromatics into high-cetane compounds. In particular, this study tried to identify the effect of coke on acid sites present on a new generation of WNiPd/$TiO_2Al_2O_3$ catalyst.

2. Experimental

2.1 Catalyst preparation and characterization

The $TiO_2Al_2O_3$ support was prepared by a controlled co-precipitation of aluminum and titanium hydroxides and calcinated in air. Small pellets of 0.001-m diameter 0.001-m length were prepared by extrusion, and the metal incorporated using two steps of incipient wetness impregnation. First, an aqueous solution of tungsten salt was added; then after drying, the solids were contacted with another aqueous solution of nickel and palladium salt. After impregnation, the solid was dried in air and calcinated at 550°C. Other details of catalyst preparation and characterization can be seen in Galiasso Tailleur and Ravigli (2005) [13].

Two identical samples of the catalyst were in turn installed in a fixed-bed micro-reactor and presulfided in situ. One of the samples was used to process 100% of LCO at standard HDT conditions during 10 weeks on stream to produce 50 ppm (low-sulfur) diesel. The other sample was used to process 100% of LCO to produce 15 ppm (ultra-low) sulfur diesel during 10 weeks' operation. The shutdown of the microplant and download of catalyst procedures were previously developed and used for other catalysts. The methodology eliminates the adsorbed hydrocarbons in the spent samples and preserves the reduced state of the metals and the hydrocarbons content on the coke. The catalysts that were transferred

from the microreactor to the laboratory under inert atmosphere were washed in xylene for 24 hours and dried in nitrogen to constant weight. Then samples were stored under inert atmosphere in a vacuum chamber to avoid catalyst reoxidation. The solids were analyzed using the following techniques:

- **Physical method**. Surface, pore volume, and average pore diameter were measured using standard nitrogen adsorption (Micromeritics 250) and mercury porosimetry methods.
- **CH_2Cl_2 extraction and GC-MS analysis.** Deactivated catalysts samples, after being washed with xylene, were extracted in a column packed with the powder of the catalyst by elution with dichloride methane. The elute material was concentrated by evaporation and then injected in a GC-MS system comprising an HP 5890 Series II, HP-5 column (internal diameter 0.28 mm and length 20 m with inner surface coated by methylsiloxane), and HP 5972 mass spectrometer. A 1μl sample was injected twice for every catalyst sample. The whole spectrum is used as a fingerprint to characterize "soluble" coke. In the MS signal, 70% of the compound composing of the sample was identified using pure molecules and the mass spectrometry library (National Institute of Science and Technology). The elemental analysis of the insoluble coke remaining on the surface was performed by dissolving the inorganic matrix with fluorhydric acid, washing the remaining solid with water and ether, drying in nitrogen and analyzing the carbonaceous solid.
- **Chemical characterization.** C, H, and N were determined by a LECO (D5373) carbon analyzer and sulfur by a XRF (D1757) and reported in wt%.
- **Solid ^{13}CNMR spectra.** The analysis of the carbon deposited on solids was performed using a Varian spectrometer operating at a frequency of 50.576 MHz, with cross-polarization using adamantine as reference. The technique allowed us to detect the amount of aromatics and paraffinic type of carbon present on the surface. The signals were recorded, deconvoluted, integrated, and their relative amount calculated for further analysis.
- **TPO.** The samples of catalyst were subject to temperature-programmed oxidation (TPO) using a PerkinElmer TGA 8 system with a gas mixture containing air (35ml/min) in helium at a linear heating rate of 10°C/min between 30°C to 600°C. The CO_2 and SO_2 produced were recorded as a function of time.
- **Pyridine TPD**. Pyridine thermal programmed desorption (TPD) analysis was used to characterize the total acidity strength of deactivated catalyst and FTIR analysis to determine the Bronstead and Lewis content. For that a McBain microbalance with a 1-mg sample (thin layer) that is transferred into on purpose-built IR cells was employed. The catalysts were pretreated with argon (3 liter/minute) until achieving a constant weight using a program of 10°C/minute to increment the temperature from 30°C to 200°C or 300°C; weight losses were recorded. After reaching peak, the temperature was kept constant at 200°C or 300°C for 2 hours, and then cooled at a rate of 10°C/minute. A stream containing pyridine (0.001 molar) diluted in argon was passed through the catalyst at room temperature (30°C) for 2 hours. After that, pure argon was flowed at the same temperature for another two hours. The catalyst sample was then characterized by FTIR spectroscopy (main bands: Lewis at 1445 cm^{-1}; Bronstead at

1540 cm^{-1}. Adsorption intensities were calibrated using the internal standard and compared with those of fresh catalyst.

- **CO adsorption.** Pd dispersion was measured using the same IR equipment used for pyridine adsorption. CO reactant (Linde) was at 99.99% purity. The solids were compressed in a thin layer film and dried in argon at 350K, 1000 Pa for 3 hours. Then cell was evacuated to 13 Pa at room temperature before the FTIR measurements were started. The metallic function was characterized by stepwise adsorption of small doses of carbon monoxide at room temperature until saturation was achieved at 990 Pa (200 scans with 2 cm^{-1} spectral resolution).
- **XPS.** A Bruker 300 apparatus (Al cathode) using Al-Kα 1486.6 electron volts (eV), and with 200W of power was used. For peak area measurements, a Shirley-type integral background was used [14]. When multiple components were present under a given XPS envelope, a non-linear least-square-curve-fitting routine was implemented (Levenberg-Marquardt damping method). All peaks were fitted using a Voight function with 20% Lorentzian character. Curve fitting of the W_{4f} region (42–32 eV) was carried out according to the methodology described by Galiasso T., 2007 [13]. The XPS parameters (peak position, peak width) relative to W^{+4} were obtained by curve fitting the spectra of the oxide samples. These parameters were kept constant when fitting the spectra of sulfide specimens. The parameters for the "sulfide" species were obtained by curve fitting the sample sulfide at 375°C and allowing the peak position and FWHM to relax into their local minimum. The results were reported as exposed $I_W/(I_{Ti}+I_{Al})$ and $I_{Ti}/(I_{Ti}+I_{Al})$.The dispersion was analyzed using different angles of beam incidence on the sample to check the coke attenuation of the signals.

2.2 Feed and product characterization

- **Analysis of the feedstock and HDT products.** The LCO was characterized using a programmed temperature GC technique coupled with a low-intensity mass spectrometry method. In parallel, a preparative HPLC was also performed using a hexane carrier and an ultraviolet detector. The eluted fractions with toluene and methanol were analyzed using a LECO elemental analyzer, ^{1}HNMR spectroscopy (Varian 400-MHz spectrometer, 10-mm broadband probe), alumina percolation method (using tetrahydrofuran as solvent), and mainly a high-resolution mass spectrometry (HRMS–Philips 2341). In this way, it was possible to analyze families of aromatics, naphthenes, and paraffins. The cetane number was determined by using the D613 ASTM method.
- **Microplant long run tests.** The microplant has a conventional isothermal downflow fixed-bed reactor [11]. Two parallel tests were performed. Both were operated at a temperature variable from 350°C to 378°C, 4 (molar) of H_2/HC ratio, and 12.5 MPa of total pressure during 10 weeks. In one of them $0.2h^{-1}$ space velocity were used to produce a 50 ppm sulfur product, and in the other a 0.1 h^{-1} space velocity was used to generated a 15 ppm sulfur product. The $WNiPd/TiO_2Al_2O_3$ catalyst was loaded in the reactor diluted with 50% of inert material. The catalyst was pre-activated in situ with straight-run light gas oil spiked with 1% of CS_2 at 300°C for 6 hours. Then the microreactor was started up with LCO and operated continuously for the 10 weeks on stream at the operating conditions mentioned above, generating two spent catalyst

samples at the end of cycle. These catalysts were called Spent 1 (used to produce 50 ppm sulfur) and Spent 2 (used to produce 15 ppm sulfur fuel). During the tests, duplicate samples of hydrotreated LCO were taken daily, and mass balance was performed to check the operation. Having achieved the period on stream, the catalysts were cooled down to 200°C, washed with xylene for a half day, and then dried with nitrogen at 200°C for another half day. The catalysts were ready to be tested using the synthetic feed.

- **Test with synthetic feed (probe molecules).** The spent catalysts were tested using a blend of 30% of methyl-naphthalene, 10% of methyl-tetralin, and 1.5wt% of sulfur as dibenzothiophene in hexadecane (Feed 2). The temperature needed to obtain the 15 ppm of sulfur in the product were 340°C on fresh, 372°C on Spent 1, or 380°C on Spent 2, and the other operating conditions were 0.5 h^{-1} of LHSV, 4 H_2/HC molar ratio, and 12.5 MPa of pressure. Other space velocities were also explored for Spent 1 catalyst at 372°C and for Spent 2 at 380°C. Finally, the catalysts were washed by continuous pumping of xylene at 200°C for 24 h, dried in nitrogen for another half day (120°C) and discharged in a dried-inert chamber. The two samples of spent catalyst were then characterized.

3. Results and discussions

The main objective of this study was to demonstrate the variation in nature and composition of coke obtained during the processing of LCO and its effect on catalytic active phases. The spent catalysts were characterized by a combination of different analytical techniques to obtain the composition of coke deposits and the characteristic of acid sites. As shown in Table 1, carbon content in spent catalysts was in the range 6.4 wt%, and the H/C ratio (wt) was 1.09 in Spent 1, and 1.08 in Spent 2. The hydrotreating temperature was adjusted to keep constant at 99.66% or 99.9% during 3 months in operation. The difference in sulfur conversion seems to be minor, but required 10^{o}C higher temperature at the beginning of the cycle and 14^{o}C at the end of cycle to treat the LCO to low-sulfur (50 ppm) or to ultra-low-sulfur diesel (15 ppm), at constant other operating variable. During this period on stream the paraffin, naphthene, and aromatics content seem largely affected, as was the nature of coke deposition, a cause of catalyst deactivation. Therefore, to optimize the level of conversion and the catalyst composition for future commercial operation, it is imperative to know the impact of coke deposits on the active sites. To start, the catalyst and the coke were characterized.

3.1 Catalyst composition and physical properties

The fresh catalyst before sulfiding contains 15% WO_3, 5.3% NiO, and 0.2% by weight of PdO oxide species; they are reduced and sulfided in situ to generate the metal active phases. The support contains 10 wt% of TiO_2 in γ-alumina. This support was treated with steam-ammonia to achieve the Ti migration into the aluminum on surface to build a particular distribution of acid strength, according to analysis done with XPS, FTIR, and ^{29}AlNMR, information that was discussed previously [12]. The information for fresh catalyst is included in Table 1 as a reference, but the discussion will focus on spent catalyst that had accumulated coke during the three months on stream. Both present completely different on-surface properties than fresh catalyst. During the first week in operation with 100% LCO to produce low sulfur diesel component (not included here; see detail in ref. [13]) the catalyst lost around 41% of the surface and 55% of micropores. Now, Spent 1 has ~5% higher

micropore volume and surface area than Spent 2, an insignificant dissimilarity, in agreement with the relative low difference in total coke (~5%) content. The same small difference is observed in total sulfur content (~4%), as well as in total H/C ratio (3%), but macropore volume and the amount of insoluble coke are approximately the same in both samples. The main difference between both samples is in the soluble coke content, which is 18% higher in Spent 2 than in Spent 1, and this amount represents around the 15% of the total coke content.

Table 1. Physical and chemical properties of catalysts.

Properties	Fresh	Spent 1	Spent 2
Surface m^2/g	245	112	103
Micropore vol. cm^3/g	0.17	0.08	0.075
Macropore vol. cm^3/g	0.35	0.29	0.27
Total sulfur wt%	5.6	6.1	6.3
Total carbon wt%	-	6.2	6.4
Soluble carbon wt%	-	0.99	1.11
C/H/S soluble carbon w%	-	91.0/ 7.66/ 1.34	91.2/ 7.39/1.41
C/ H/S insoluble carbon w%	-	91.5/ 7.13/1.24	91.7/ 6.89/1.31

Soluble coke composition. Table 2 reports the concentration on the main polyaromatic hydrocarbons identified by mass spectrometry on the soluble coke extracted by CH_2Cl_2 from Spent 1 and Spent 2 catalysts.

Table 2. Polyaromatics composition in soluble coke

Compound wt %	Spent 1	Spent 2
Naphthalene	1.5	0.5
Fluorene	13.5	12
Phenantrene	2.2	3.1
Anthracene	9.1	7.9
Fluoranthene	1.2	2.4
Triphenilene	22	23
Pyrene	0.5	1.6
Chrysene	18	16
Benzo(a)anthracene	3.5	5.1
Benzo(g,h.i)fluoranthene	1.5	0.5
Benzo(k)fluoranthene	0.3	0.1
Perylene	--	0.1
Benzo(a)perylene	-	-
Dibenzo(a,h) antracene	2.4	2.0
Other	24.6	26.3

The identification of these polyaromatic hydrocarbons is based on determining the retention time obtained for various model polyaromatic hydrocarbons used as reference. The main compounds observed in soluble coke are: fluorene, anthracene, and fluoranthene that account for more than 50% of total hydrocarbons, exclusive of some amounts of triphenylene and chrysene. A total of 25% of the hydrocarbons could not be identified due

to unavailability of suitable reference model compounds. In Spent 2, similar types of compounds than those found on Spent 1 soluble coke are present, but in different proportions. Both extracts contain a low H/C ratio, as well as some small amount of sulfur compounds. The nature of this soluble coke in the two hydrotreating catalysts differed from those analyzed on catalyst used for the hydrodesulfurization of residue by Sahoo *et al.* [15, 16]. They reported differences in the soluble coke attributed to the composition of the feed processed in commercial unit. Here, the difference between Spent 1 and 2 soluble cokes is due to the severity in the hydrotreating operation used to achieve the sulfur target in the product; similar effect of severity was reported by Martin *et al*. [17] for reforming type catalyst.

^{13}CNMR analysis. Two deactivated samples before (BE) and after (AE) extraction with CH_2Cl_2 were analyzed by CP/MAS. The majority of the coke is an insoluble type located in clusters on the solids (TEM analysis not shown). The coke clusters are mainly composed by condensed polyaromatics that seems to surround the metallic areas (micro-difraction). The ^{13}CNMR was employed to evaluate the degree of aromaticity in both soluble and insoluble cokes. Figures 1a and 1c show that both samples contain an intense aromatic band at -135.0 ppm that is accompanied by two other small bands at 125 ppm and 152 ppm attributed to aromatic coke. Other small bands between 30 ppm and -50 ppm are assigned to aliphatic coke [18-19]. The ratios of intensities between these peaks are:

Spent 1 $\frac{I_{152}}{I_{135}}=0.45$; $\frac{I_{105}}{I_{135}}=0.05$; $\frac{I_{30}}{I_{135}}=0.08$ before extraction (BE)

Spent 1 $\frac{I_{152}}{I_{135}}=0.67$; $\frac{I_{105}}{I_{135}}=0.02$; $\frac{I_{30}}{I_{135}}=0.03$ after extraction (AE)

Spent 2 $\frac{I_{152}}{I_{135}}=0.41$; $\frac{I_{125}}{I_{135}}=0.15$; $\frac{I_{30}}{I_{135}}=0.08$ before extraction (BE)

Spent 2 $\frac{I_{152}}{I_{135}}=0.71$; $\frac{I_{125}}{I_{135}}=0.01$; $\frac{I_{30}}{I_{135}}=0.02$ after extraction (AE)

Spent 2 shows higher aromaticity (152/135 bands ratio) and broader distribution than Spent 1 (before extraction). In the two spent catalysts, the aromatic band is quite broad due to the heterogeneous distribution of aromatic species present in the coke and with different degrees of alkyl substituents content. Some efforts were undertaken to evaluate their aromaticity using cross-polarization; data about the parameters are published in reference [16]. The time-dependent evolution of carbon magnetization during polarization transfer is higher for Spent 2 before extraction indicating more complex bonding configurations and motional constrains than in the Spent 1 (before extraction) sample. After extraction, a similar type of spectra is observed for both samples characteristic of an aged coke already observed in other hydroprocessing spent catalysts. The operating condition during the initial deposition of coke—that leads to most of the insoluble coke—was similar in both samples.

The calculation of aromaticity alone does not give enough information to describe the average coke molecule; more quantitative information pertaining to different types of protonated and non-protonated (bridgehead) aromatic carbons is needed. The work to consider the difference in magnitude of dipolar coupling between aromatic carbons, which are attached to protons, and quaternary carbons is underway, but the preliminary results

indicate that coke in Spent 1 is more protonated than Spent 2, in agreement with the H/C ratio. In summary, there are some important differences in amount and type of soluble coke, and a slight one in insoluble coke between the two samples. Following is an explanation of how these differences in the coke affect the oxidation behavior.

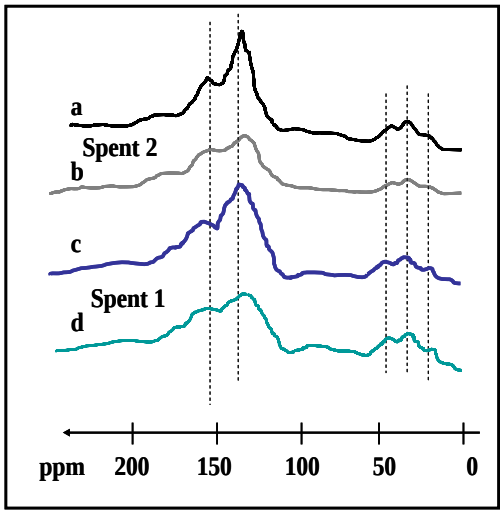

Figure 1. ^{13}CNMR analysis of coke before (a and c), and after (b and d) extraction

TPO of soluble and insoluble coke. Thermal oxidation analysis of the spent catalysts, before and after extraction, is shown in Figure 2. The amount of CO_2 released by the sample as a function of temperature gives information about the nature of the coke. Three different regions were recognized previously by Barbier *et al.* [20] and Parera *et al.* [21], among others, for reforming spent catalyst and extensively used in the literature for characterization of coke: (1)150°C–250°C oxidation of high-in-hydrogen coke present on metals; (2) 300°C–400°C oxidation of coke located on the support near the metal, which contains some hydrogen, and (3) 450°C–520°C oxidation of highly aromatic coke deposited on the support. In parallel, the amount of SO_2 released by the sample was measured, as was the amount of hydrogen oxidized quite quickly into water at low temperature. The ratios of the integrated area of the three CO_2 peaks are:

$$\text{Spent 1}\ \frac{I_{250}}{I_{360}}=0.17\ ,\ \frac{I_{470}}{I_{360}}=0.12\ \text{(BE)};\ \frac{I_{250}}{I_{360}}=0.09\ ,\ \frac{I_{470}}{I_{360}}=0.19\ \text{(AE)}$$

$$\text{Spent 2}\ \frac{I_{250}}{I_{360}}=0.16\ ,\ \frac{I_{470}}{I_{360}}=0.10\ \text{(BE)};\ \frac{I_{250}}{I_{360}}=0.10\ ,\ \frac{I_{470}}{I_{360}}=0.21\ \text{(AE)}$$

The ratios of the area (I) of the peaks of CO_2 released at different temperatures by the samples indicated that around 50% of the carbon is burned at 360°C in both samples, but the Spent 1 catalyst presents a lower amount of coke that combusted early in the process - at 250°C - than Spent 2 catalyst. The difference might be associated with the soluble carbon on metals. After extraction, the amount of coke that is burned at 250°C and 360°C is reduced in

both samples, but the quantity of graphitized coke that is oxidized at 470°C is quite similar in both catalysts, before and after extraction.

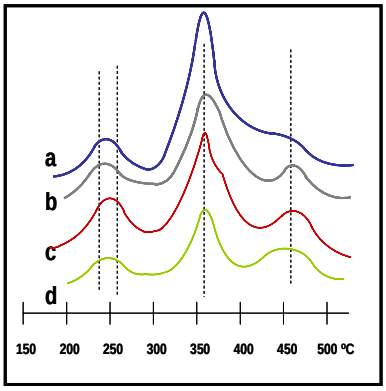

Figure 2. TPO-CO_2 from Spent 1 and Spent 2 catalysts before extraction (**a**, **c)** and after extraction (**b**, **d)**, 10°C/min

This information, together with previous ^{13}CNMR analysis, indicated that graphitized coke is formed during the startup (first week) on the support and was "aged" as a function of time on stream. The main difference between the samples is in the coke influenced by the metals. In particular, this catalyst contains Pd, which seems to help the combustion during the TPO, because the carbon combustion starts at lower temperatures for all the peaks than those reported in the literature for deactivated $NiMo/Al_2O_3$ catalyst [22].

SO_2 is formed by combustion of sulfur species at low temperature (between 230°C and 260°C, Figure 3b and 3c); no further SO_2 produced at 330°C. Most (90%) of sulfur species comes from the sulfide linked to the metals, and the TPO provides little information about the nature of the sulfur in coke itself. The combustion of the fresh catalyst without coke presents a different pattern (one peak at 200°C with a long tail and a second peak at 350°C, Figure 3a) respect to the Spent 1 catalyst (Figure 3b); the difference between them is associated with better access of oxygen to the metals that contain the sulfur in the fresh catalyst. Spent 1 and Spent 2 presents similar rate of sulfur combustion (Figure 2b v. 2c). The spectra do not provide additional information. The combustion of insoluble coke (after dissolution of the support on HF) presents a very different pattern. Combustion starts around 200°C and shows two peaks, but the rate of coke combustion might be limited by the oxygen accessibility to the internal layers, since the insoluble coke is mainly a non-porous solid. It did not contain metal sulfides (less that 0.1%). In addition the TPO of Spent 1 and 2 insoluble cokes performed at half of heating rate (5°C/min instead of 10°C/min) show that the rate of SO_2 production is not affected by the rate of carbon burning. By doing that the sulfur starts to be oxidized at lower temperature, while those for carbon burning remain mainly unaffected. It can be said that around 65% of sulfur in insoluble coke is combusted at low temperature and might be present in coke located near the metals, while the rest burns at higher temperature and can be present in the turbostratic type of coke. Clearly, the sulfur is present in soluble coke in a sort of polymeric aromatic structure that could not be identified in this study by MS analysis.

Now, the characteristic of the active surface will be discussed

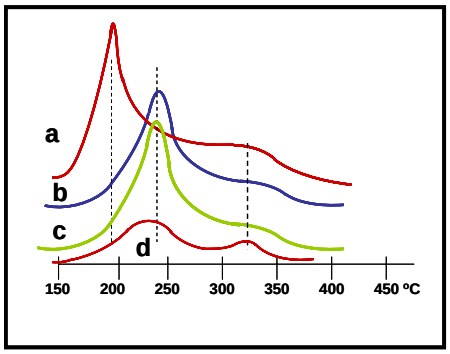

Figure 3. TPO-SO_2 for (a) fresh, (b) Spent 1, (c) Spent 2, (d) insoluble coke Spent 1

Metals - XPS dispersion. The fresh catalyst presents the characteristic XPS signal due to W_{4f}, Ti_{2p}, and Ni_{2p} after having been sulfided. The spectra (binding energies and bandwidth of W, Ni and S species in fresh catalyst were reported previously [13]. The sulfided $NiWPd/TiO_2A1_2O_3$ catalyst exhibits only one sulfur peak at about 161.6 eV, which corresponds to S^{2-} [23, 24] species. According to the literature [23] and references therein, the W_{4f} doublet lines at 32.0 and 34.1 eV correspond to W^{IV} species in a WS_2-like structure, while the small bands at 35.5 and 37.5 eV are assigned to no reduced W^{VI} in an oxygen environment. In order to estimate the fraction of sulfided W species present on the fresh and spent catalysts, the intensity of W_{4f} XPS signals were fitted assuming only the presence of (WS_2) species and reported with respect to intensities in the bands of Ti and Al. Full-width for W^{IV} signal at half maximum (FWHM) is 1.6. The fresh catalyst exhibits a Ni2p signal at 853.6 eV associated with NiWS phase shift by the Ni promotion to the WS neighbor. The Ni peaks are slightly asymmetric, and the FWHM is 1.2, indicating that the Ni species present in these samples are mostly involved in the $NiWS_x$ state, but there is some contribution of segregated NiS_x species. The XPS signal of titanium shows the presence of two species (Ti_{2p} at 463.3 eV and 463.6 at eV) attributed to Ti^{IV} acid sites with different oxygen environments [13, 24-27]. The distorted O_{1s} signal at 531.4 eV shows the presence of a shoulder at 530.2eV, probably associated to the Ti species mentioned above. In addition, there are no signals other than those of gamma alumina in X-ray diffraction between θ=45° to 60°, which may be attributed to appreciable rutile or anastase concentration. The presence of Ti and Pd affects W and Ni dispersions and the degree of sulfiding of the cluster on surface, as it was previously demonstrated by ESR and XAS, and XAFS studies [26].

Following this brief description of the fresh catalyst, we can study the spent samples. Samples containing coke were analyzed by XPS using different beam incidences to check the potential effect of coke on attenuation of the signal. Dispersion of the different elements was calculated by integrating peak areas for each of the metals detected, regardless of the phase in which they were placed (Table 3). Analysis of the spectra indicated less than 5% change in the signal ratio, and broadening of W, Ni, and Ti species occurred in coke samples. Thus, no

particular shift in the signals can be attributed to the presence of new species (built up by oxidation or migration), but all of them are broadened in presence of coke (between 0.1 and 0.2 eV).

Table 3. XPS. Dispersion of the metal phase (BE-AE)

Ratio of intensity	Fresh	Spent 1	Δ%	Spent 2	Δ%
		BE AE		BE AE	
$I_W/I_{Ti}+I_{Al}$	4.2	2.34 – 2.44	4	1.99 – 2.12	6
$I_{Ni}/I_{Ti}+I_{Al}$	2.3	1.1 – 1.3	18	1.2 –1.25	4
$I_{Ti}/I_{Ti}+I_{Al}$	7.8	4.3 – 4.5	5	3.8 - 4.1	8
$I_S/I_{Ti}+I_{Al}$	1.1	0.72 – 0.87	20	0.66 -0.77	

Around 40% reduction in XPS metal "accessibility" by the coke loading was observed between spent and fresh catalysts, and most of that occurred at the beginning of cycle [12]. Now, Spent 1 and Spent 2 metal dispersion—containing comparable amounts of coke—would present similar, if any, XPS signal attenuation (Table 3). Clearly the "accessibility" of W, Ni, and Ti is higher on the Spent 1 surface than on Spent 2 before and after extraction (Table 3 left and right values) for the same bulk-metal content. Note that in this comparison, the extraction of soluble coke increments the metals accessibility in different ways in the two samples. The variation in spent catalyst, shown in Table 3 as Δ%, is higher for S, W, and Ti, and lower for Ni species in Spent 2, than in Spent 1. These results suggest that soluble coke might be adsorbed on metal sites in different way in these two samples. Since the same initial on-surface structure was present on both samples, the difference in soluble coke structure is affected by the temperature at which this metal (and acid sites) operate in Spent 1 and in Spent 2 during the 3 months on stream. Thus, the polymerization reaction of adsorbed polyaromatics was in some way better controlled by hydrogenation operating at 50-ppm temperature, than at 15-ppm, for the same hydrogen partial pressure.

The important role Pd plays in hydrogenation is examined below. Figure 4 shows the IR spectra of CO adsorbed on Spent 1 (a) sulfided fresh catalyst (b) at 300K, and 100 Pa of CO partial pressure. A detailed study has been performed with WS_x/support, NiS_x/support, and $WNiS_x$/support (where x represent a non stequiometric sulfur compounds). Four bands of adsorbed CO appeared at 2190, 2156, 2118 and 2066 cm^{-1}, and were observed in the WSx/support sample, the intensity of which increases with the CO partial pressure. The first two bands are assigned to CO associated with Lewis acid sites and CO adsorbed on hydroxyl groups on the titania-alumina support. The second two with CO-WS_x clusters [23]. At 30 Pa of CO partial pressure the main IR band is at 2118 cm^{-1}. Increasing the amount of CO in the system caused the band at 2066 cm^{-1} to rise. At 300 Pa of CO partial pressure, the main band was that of 2156 cm^{-1}, and a shoulder appeared at 2136 cm^{-1} due to CO physisorbed. At this point, the CO adsorption on $NiS_x/TiO_2A1_20_3$ catalyst showed a band at 2097 cm^{-1} due to NiS_x sites, besides the two adsorption bands described for the support. By increasing the CO partial pressure, both the 2097 cm^{-1} peak and that of 2190 cm^{-1} increased. In $Pd(S)/TiO_2AL_2O_3$ the presence was observed of two small bands, 2060 cm^{-1} and 1910 cm^{-1}, and two large bands, 2182 cm^{-1} and 2159 cm^{-1}. The first set is attributed to CO-Pd^0, and the second set to Pd^{+2}CO in a terminal and bridging adsorption, respectively. These bands grew proportionally to CO partial pressure until 1000Pa. On the $WNi_x/TiO_2A1_2O_3$ sample, all absorption was attenuated, and absortions at 2118, 2095 and 2066 cm^{-1} were slightly shifted

up. New bands at 2095, 2078 and 2058 cm^{-1} appeared due to the NiW interactions [28]. The assignments of CO bands became more complex due to the presence of NiS, WS_2, and NiWS phases demonstrated by the XPS results. The same results were observed by other authors [29] on a WNi/Al_2O_3 catalyst.

The IR spectra of CO adsorbed and recorded on the sulfided fresh catalyst shows a very complex contribution of different species (Figure 4b). It presents a main signal due to Bronstead sites (2157 cm^{-1}), and shows an overlap in the at top CO-Ni^{2+} and CO-Pd^{2+} adsorption bands at 2100 and 2095 cm^{-1}, respectively; it also depicts important bands at 1952 and 1986 cm^{-1} attributed to a bridged CO-Pd^{2+} in a distorted environment (Pd^{2+} located in border of WNiS clusters). The complexity of the spectra make difficult to draw clear conclusions with the contribution of W and Ni bands in spent catalyst, but the CO-Pd^{2+} bands mentioned above dominate the spectra, and can be used for the analysis of the accessible Pd and PdS_x species. These bands were verified at 0.5% of Pd content on catalyst, and they increase proportionally to the CO partial pressure up to 700 Pa. In contrast, most of the well defined bands present in fresh catalyst disappeared in Spent 1 catalysts and appeared other bands assigned to the aromatics compounds present in coke deposited on surface (Figure 3b). Other signals due to coke that appeared in the 1200–1800 cm^{-1} region are discussed below. The best definition for the CO-Pd and CO-OH bands in deactivated catalysts was obtained at 100Pa of CO partial pressure and 300 K of temperature.

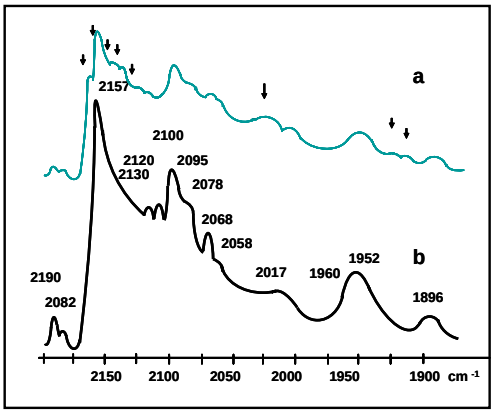

Figure 4. CO adsorption on Spent 1 (a) BE, and fresh (b) catalyst (300Pa, 300K) (Ref 27)

The ratios of main bands in Spent 1 and 2 catalysts, before (BE) and after extraction (AE) catalyst are as follows:

$$\frac{I_{Spt1}}{I_{Spt2}} = 1.23(B:2157); \frac{I_{Spt1}}{I_{Spt2}} = 1.13(L:2190); \frac{I_{Spt1}}{I_{Spt2}} = 1.05(Pd:2096) \quad ; \text{(BE)}$$

$$\frac{I_{Spt1}}{I_{Spt2}} = 1.05\ (B:2157); \frac{I_{spent1}}{I_{spent2}} = 1.01\ (L:2157) \frac{I_{Spt1}}{I_{Spt2}} = 1.02(Pd:2096) \quad ; \text{(AE)}$$

The results indicate that the main difference in the signals, obtained for CO at this adsorption conditions before the extraction, were the larger number of CO-accessible sites in Spent 1 than those in Spent 2. The main difference between the samples is observed in the number of Bronstead (B) sites; the Lewis sites (L) shows less variation. After extraction, the number of acid- and metal-accessible sites seems to be quite similar for both solids; therefore, this aged insoluble coke seems to be formed on the same type of sites at the startup operation in both samples. The soluble coke is apparently adsorbed on some Pd metal sites, since its removal by extraction promoted a 10% higher CO adsorption on Pd. The larger number of CO-accessible Pd-content sites in Spent 1 than in Spent 2 confirms its potential to better control the polymerization reaction in the first than in the second catalyst...

Now, pyridine adsorption is discussed to confirm the effect of soluble coke on acid sites.

Pyridine adsorption. Pyridine adsorption studies were performed with sulfided catalysts. The spectra of pyridine adsorbed on fresh catalyst reveals the presence of Bronstead (1548 cm^{-1} and 1649 cm^{-1}) and strong Lewis (1633 cm^{-1} and 1455 cm^{-1}) acid sites [12, 28-31]. The spectrum of Spent 1 and Spent 2 catalysts before extraction are shown in Figures 5a and 5c; they present a typical band at 1600–1610 cm^{-1} that is generally proportional to the amount of coke [30] on top of the acid bands mentioned on fresh catalyst. The 1600 cm^{-1} band is ascribed to highly unsaturated compounds, such as polyolefins and polyaromatics. This band increases slightly with the time on stream and is shifted toward lower wave numbers (from 1610 to 1603 cm^{-1}). Other bands at 1592, 1575, 1525, 1415, 1387, 1367, and 1348 cm^{-1}, characteristic of aromatics polymers, were observed in these two samples, and in other previously studied spent hydrotreating catalysts. These bands are indicated with arrows in the Figure 5. By comparing the Spent 1 and 2 peaks (5a vs. 5b), before extraction, it can be see that most of the bands are present in both samples with different relative intensities; nevertheless, there is some difference in bands in the region of 1350–1590 cm^{-1}. All the differences in IR signals disappeared after extraction, and the insoluble coke spectrum in both samples "looks" similar: the bands at 1606 cm^{-1} were sharply reduced and the other small signals were attenuated almost to the point of disappearing.

Pyridine was then adsorbed on Spent 1 catalyst before and after extraction (spectrums 5c and 5d). By comparing the bands attributed to pyridine, a change on acidity and a modification in the Bronstead (1548)/Lewis (1455) ratio can bee seen before and after extraction. The semi quantitative analysis of the two bands confirms the additional coverage of soluble coke to the acid sites (preferentially Bronstead sites) compared with those already blocked by insoluble coke.

$$\text{Spent 1}\ \frac{I_{BE}}{I_{AE}} = 0.91(B{:}1548\,\text{cm}^{-1}),\ \frac{I_{BE}}{I_{AE}} = 0.95(L{:}1455\,\text{cm}^{-1})$$

The results of the relative acidity measured by thermobalance at 200°C for Spent 1 and 2 (BE) are,

$$\frac{I_{Spent1}}{I_{Spent2}} = 1.11(B{:}1548\,\text{cm}^{-1}),\ \frac{I_{Spent1}}{I_{Spent2}} = 1.05(L{:}1455\,\text{cm}^{-1})$$

And at 300°C,

$$\frac{I_{Spent1}}{I_{Spent2}} = 1.15(B:1548\ \text{cm}^{-1}),\ \frac{I_{Spent1}}{I_{Spent2}} = 1.06(L:1455\ \text{cm}^{-1})$$

The Spent 2 catalyst had fewer Bronstead and Lewis sites at 200° and 300°C than did the Spent 1, before and after extraction, but the effect of coke is more noticeable on Bronstead than on Lewis sites. The mol of adsorbed pyridine at 200°C minus the mol adsorbed at 300°C is defined as number of weak acid sites (B + L), while those adsorbed at 300°C (B + L) as number of strong acid sites; both samples show higher number of weak than strong sites, before and after extraction. The effect of operating the catalyst at higher temperature (15 ppm of sulfur) than a lower ones (50 ppm of sulfur) results in a larger reduction of weak sites than strong sites. The results BE and AE confirm that soluble coke covered more Bronstead than Lewis acid sites. The Bronstead site is supposed to play an important role in the (LCO) polyaromatics polymerization reaction that generated coke (see discussion about the role of Bronstead in, for example, ref [32]), a reaction strongly dependant on the operational temperature. Therefore the higher reduction in Bronstead in Spent 1 is attributed to its higher operating temperature.

The values of the relative weak and strong acidities (ratios by weight (W) of pyridine that remain adsorbed) are:

$$\text{weak}\ \frac{W_{L+B}^{Spent\ 1}}{W_{L+B}^{Spent\ 2}} = 1.05\ ,\ \text{strong}\ \frac{W_{L+B}^{Spent\ 1}}{W_{L+B}^{Spent\ 2}} = 1.09$$

This reduction in weak and strong acid sites is associated with the soluble coke coverage of the Ti-O-Al- acid sites species detected by XPS (see above discussion on surface composition) and confirms the decrease on acidity observed in this work by CO adsorption on B and L sites.

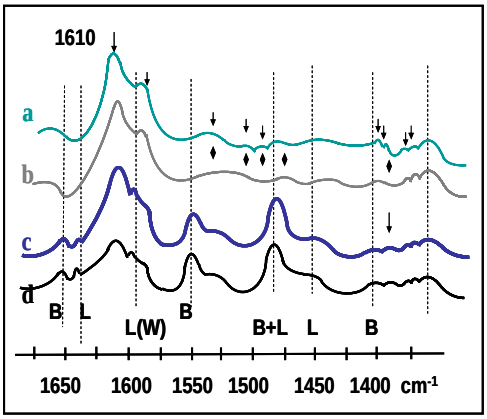

Figure 5. Pyridine adsorption on (a) Spent 1 (BE), (b) Spent 1 (AE), (c) Spent 1+pyridine (BE), (d) Spent 1 + pyridine (AE) catalysts.

Once the effects of insoluble and soluble coke on metal and acid sites' "accessibility" are established, the effect of coke on activity and selectivity can be discussed.

3.3 Activity using LCO as feed stock. Table 4 shows the properties of LCO-hydrogenated products using fresh, Spent 1, and Spent 2 catalysts. The final temperature required to obtain 50 ppm of sulfur in the products is indicated in the first row. The performance of the two spent catalysts (feed 1 columns for Spent 1 and Spent 2) show a clear deactivating pattern when they are compared with fresh catalyst. Higher temperatures (18^{o}C for Spent 1 and 26^{o}C for spent 2, respectively) were needed to obtain around 50 ppm of sulfur in the product with deactivated catalyst respect to those needed by fresh catalyst. It is important to mention that this catalyst had been previously operated with a straight-run diesel (0.5% of sulfur and 30% wt of aromatics) for 10 weeks to produce 50 ppm sulfur in the product, and the increase in temperature needed after the deactivation period was only 8^{o}C. Clearly the higher refractory sulfur and polyaromatics content present in the LCO is responsible for the faster deactivation of the catalyst, a well known fact in commercial operation of middle distillated hydrotreaters.

The conversion of polyaromatics starts by tri- and di-aromatics ring adsorption on metal sites, where they are bounded by σ or π interactions. There, they are hydrogenated to akyl-naphtho-aromatics using hydrogen molecules adsorbed (σ bond) nearby in a metallic site (or "spilled over" in the border of clusters). There adsorbed alkyl-polyaromatics can also suffer minor dealkylation (exocycle-cracking), losing its branches, as well as some hydrogenolysis of their side chains. The hydrogenated poly-alkyl-naphthenic-aromatics molecules desorbs from the metal site and migrate into the acid sites where the naphthenic ring might be protolytically dehydrogenated by acid sites, suffering a skeletal isomerization and a ring opening (endocycle cracking), to form another poly-alkyl-aromatic [33-36]. The cracking reactions of this alkyl-aromatic and alkyl-nahthenic molecules reduce the "paraffinicity" of the products and their cetane number and change the aromatic distribution along the boiling range by transferring the heavy aromatics and naphthenes into the lighter part of the diesel. A simplified scheme for the mechanism of the hydrogenation, ring opening, and cracking reactions for naphthalene is shown below in Figure 6. There has been much discussion about the role played by metal and the type of acid sites involved in the isomerization and cracking during the ring opening reaction (for example sees the discussion about this on McVicker *et al*. [37]. No attempt is made here to clarify further the role of the metal, Bronstead, and Lewis sites until additional experiments might support the point. For the present analysis it is proposed a simplified scheme where weak acid sites are used for isomerization and ring-opening reactions (sites 1), while strong ones are employed to crack the paraffins (sites 2), based on previous results [38, 39]. Figure 6 shows in the upper part the hydrogenation of the di-ring-aromatics, in the middle the isomerization and ring opening of naphthenes, as well as the production of isoparaffins (indicated by bracket and subscript $_i$), and the cracking of alkyaromatic and isoparaffins in the lower part.

In table 4-left columns, by comparing the results obtained with Feed 1 (LCO) on Spent 1 or 2 catalysts with those obtained on fresh catalyst it can be see important difference in aromatics and naphthenes concentration in products, for the same level of desulfurization First the hydrogenation of diaromatics has been decreased 33 and 44% respectively, in spite

Table 4. Products of Feed 1 & 2 as a function of time on stream.
Feed 1: LCO (LHSV 0.2h^{-1}) Feed 2: synthetic (LHSV 0.5 h^{-1})

Properties wt%	**Fresh**		**Spent 1**		**Spent 2**	
Operating Temperature °C	354		372		380	
Feed	1	2	1	2	1	2
Sulfur (ppm wt)	58	3	55	6	65	4
Nitrogen (ppm wt)	22	-	42	-	55	-
Mono-aromatics / alkyl benzenes	13	10	10	9	8	10
Di-aromatics / naphthalene (all)	9	11	12	13	14	13
Mono-naphthene / alkyl cyclohexane	9	8	7	5	6	2
Naphthen-Aromatic/ (tetralin - all)	16	11	22	13	25.5	13
Di-napththenes / (decaline – all)	22	7	20	6	19	6
Other aromatics and naphthenes	4.5	9	4.2	9.5	2.4	10
C_{10}-C_{20} paraffins	18	18	16	22	13	23
C_4-C_{10}	6	28	8	24	10	23
C_1-C_4 paraffins	2.3	5.8	3.9	6.9	4.3	7.2
Cetane number (-)	44	-	38	-	<38	-

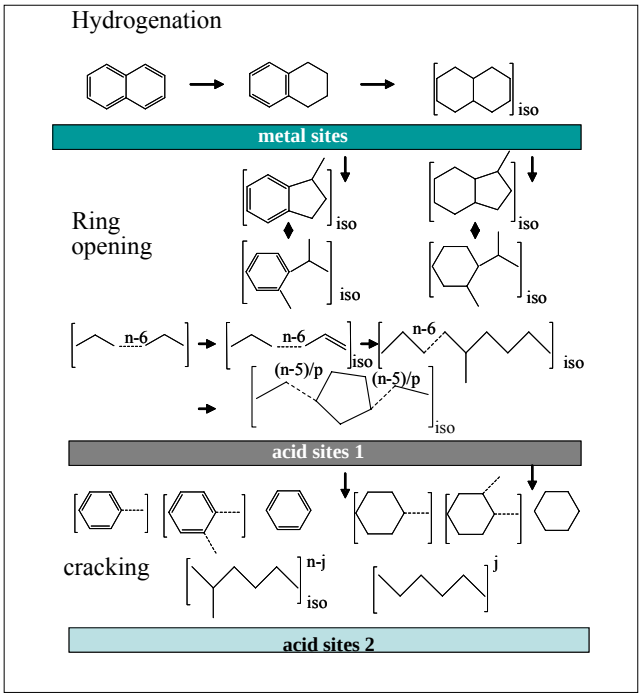

Figure 6. Paths of reactions using one metal site and two acid sites

of the temperature increment used to compensate the deactivation in sulfur removal. At the same time the production of monoaromatics were reduced in 23 and 38% and those of naphtho-aromatics incremented in 36 and 60% respectively. Clearly the production of alkylaromatics was reduced less while those of light paraffins were incremented less on Spent 1 than on Spent 2 catalyst. Table 4 confirms that cetane number is reduced by the deac- tivation of the ring opening and cracking function.

The higher the severity of the deactivation, the lower is the amount of of alkylparaffins produced boiling in the range of diesel (C_{10-20}). Without a doubt, the higher temperature used on Spent 2 catalyst reduced the alkyl-benzene and alkyl-cyclohexane generation (products of the ring opening reactions). This phenomenon can be associated with the difference in the number of weak and strong sites remaining on the surface of the solid, and to the difference in activation energies of the two competitive reactions involved. Therefore, the cetane number in the LCO produced with Spent 2 is lower than those produced with Spent 1 catalyst.

The importance of acidity on catalyst activity and selectivity was also recently noted with regard to WNi/beta-alumina catalyst for LCO upgrading [40]. To confirm the effect of coke on active sites, the spent catalysts were tested with much simpler model molecules.

3.4 Test with synthetic feed. To be able to confirm the effect of acid function deactivation, the spent catalysts were tested with synthetic feed at constant sulfur removal. Table 4-right columns shows the results. The dibenzothiophene (DBT) can be desulfurized through direct and indirect routes [41, 42], but in the presence of large amounts of aromatics, the main product of the sulfur removal is phenylbenzene (PB-direct route), in agreement with previous results [38, 39]. The PB produced by desulfurization might then be hydrogenated in competition with other aromatics, or cracked to produce benzene. The detailed analysis of

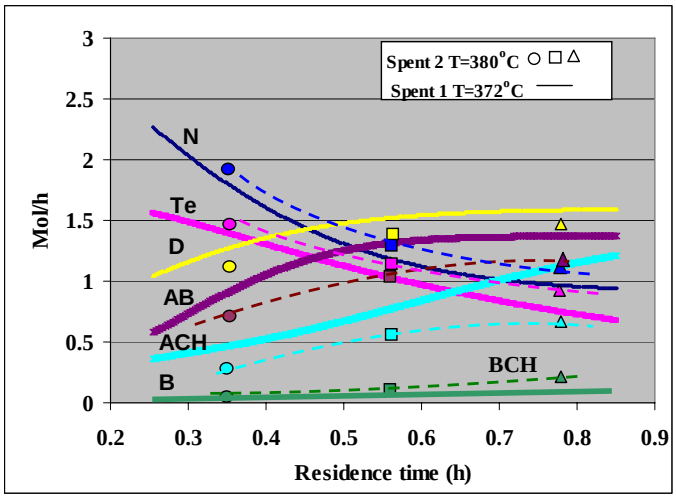

Figure 7. Effect of residence time on product distribution (Spent 1): full line, Spent 2: dashed line; circle, square, and triangle: experimental data; N: naphthalene, Te: tetralin, D: decalin, BB: butylbenzene, BCH: butyl cyclohexane, B: benzene.

the product confirms the presence of 0.5% and 0.7% by weight of cyclohexyl-benzene and cyclohexyl-cyclohexane for the fresh catalyst, but much less in the Spent 1 and Spent 2 products, due to the observed increased amount of aromatics present on the latter products. Table 4 -left columns show that fresh catalyst is able to produce a quite fast conversion of the naphthalene into tetralin and then into decalin. (Table 4, Feed 2) confirms a decrement in the intermediaries (Te and D) in products obtained with deactivated catalyst in spite of the rise in temperature used to compensate the deactivation of hydrodesulfurization. The fact that there was larger amount of benzene and a negligible amount of cyclohexane formed on spent catalyst products than in the fresh catalyst is the result of the isomerization (weak acid sites) and dealkylation (strong acid sites) deactivation. Table 4 shows that the amount of ring-opened products (alkylbenzenes and alkyl-cyclo hexanes) decreases and the amount of dealkylated compounds (other aromatics and naphthenes) increases with the deactivation.

The pilot plant results obtained with Feed 2 at three different residence times that generate products with 500, 50, and 10 ppm of sulfur from synthetic feed using Spent 1 (T:358°C) or Spent 2 (T:370°C), are shown in Figure 7. The model previously developed with fresh catalyst, was used, after adjusting the rate constants, to simulate the yield of product for deactivated catalyst. The experimental points obtained on Spent 1 catalyst, and the results of the model prediction are represented in Figure 6 as a full line. The data obtained for Spent 2 catalyst are superimposed on the same figure using dashed lines to shows the differences in the behavior. By comparing the full lines and the dashed line; it can be seen that there is a small variation between Spent 1 and Spent 2 catalysts in the hydrogenation products (Te and D) while they present an important difference in the ring-opening products (AB, ACH) and in cracking ones (B, CH). That is due to deeper deactivation in acid sites than in metal sites. The lower amount of ACH and AB, and the higher amount on B and CH in the product obtained on Spent 2 than in those produced on Spent 1 is indicative of the difference in weak and strong acid sites present on the catalyst, in accordance to the pyridine adsorption results. As it was mentioned, the additional deactivation of active sites on Spent 2 respect to Spent 1 catalyst is due to the higher temperature required for producing 15 ppm instead of 50 ppm of sulfur. That reduces the strong sites (see acidity measurement) more markedly than the weak sites. In spite of that difference in sites deactivation, the higher activation energy of the cracking reaction (17 kcal/mol) than that of isomerization (13 kcal/mol) compensates, at the end of cycle, by temperature the higher deactivation of the strong acid sites than weak ones.

Conclusions

The deactivation of a $NiPd/TiO_2Al_2O_3$ catalyst that occurred during 10-week operation to produce either 50 ppm (Spent 1) or 15 ppm (Spent 2) of sulfur in the hydrotreated LCO were studied. The results indicated that:

- There are higher amounts and more aromatics-type of “soluble” coke deposited on Spent 2 than on Spent 1 catalyst, while the amount of insoluble coke is similar in both of them.
- The metal sites are reduced in both samples with respect to the fresh catalyst. The two deactivated samples present different ratios of XPS-accessible metals and Bronstead and Lewis acid sites.

- Before extraction with CS_2, Spent 2 shows lower metal dispersion, strong/weak acid sites, and Bronstead/Lewis ratios than Spent 1. Soluble coke is the main agent responsible for that. After extraction the dispersion and acidity increase in both samples.
- The coke deposited on Spent 2 catalyst reduce more markedly the relative rates of reaction of ring opening, cracking, and hydrogenation than those deposited on Spent 1; therefore, the quality of the hydrotreated diesel is reduced by the severity of the operation used to produce 10 ppm of sulfur instead of 50 ppm during the operational cycle.

References

[1] Topsøe H., Massoth F.E., Clausen B.S., Hydrotreating catalysis, (1996) J. Anderson, M. Boudart (Eds.), *Catalysis-Science and Technology*, 11, Springer, Berlin.
[2] Murali Dhar G., Shrinivas B.N., Rana M.S., Manoj K., Maity S.K., (2003), *Catalyst Today*, 86, 45-60
[3] Bej Sh K.; (2004) *Fuel processing Technology*, 1503 -1517
[4] Ancheyta-Juarez J., Aguilar Rodriguez E., Salazar Sotelo D., Betancourt River G., Leiva-Nuncio M., (1999) *Applied Catalyst, A: General*, 180, 95-205.
[5] Song Ch. and Ma X., (2003), *Applied Catalysis B: Environmental*, 41, 1-2, 207-238
[6] Vogelaar B.M., Steiner P., Dick van Langeveld A., Eijsbouts S. and Moulijn J.A. (2003) *Applied Catalysis A: General*, 251, 1, 85-92.
[7] Muegge B.D. and Massoth F.E.; (1991), *Fuel Processing Technology*, 29, 1-2, 19-30
[8] Ramaswamy A.V., Sharma L.D., Singh A., Singhal M.L. and Sivasanker S., (1985), *Applied Catalysis*, 13, 2, 311-319.
[9] Koizumi N., Urabe Y., Inamura K., Itoh T. and Yamada M., (2005), *Catalysis Today*, 106, 1-4, 15, 211-218
[10] Weisman J.G., Edwards J.C.. (1996), *Applied Catalysis A: General* 142, 289-314.
[11] Galiasso Tailleur R.., Preprint of ISAHOF 07 Congress, Mexico, June (2007), accepted for *Catalysis Today* (2007).
[12] Galiasso Tailleur R, "$WNiPd/TiO_2Al_2O_3$ catalyst deactivation during the upgrading of LCO". (2007) accepted for *Applied Catalysis A: General*
[13] Galiasso Tailleur R., and Ravigli Nascar J., (2005) *Applied Catalyst A: Gen*. 282, 1-2, 227-235.
[14] Briggs D. and Seah M.P. (editors), "Practical surface analysis by Auger and X-ray spectroscopy", John Wiley, (1987), p. 511-32.
[15] Sahoo S.K., Ray S.S., Singh I.D.. (2004), *Applied catalyst A: General* , 278, 83-91
[16] Sahoo S.K., Rao P.V.C., Rajeshwer D., Krishnamurthy K.R., Singh I.D., (2003), *Applied Catalyst A: General*, 244, 311-421.
[17] Martín N., Viniegra M., Zarate R., Espinosa G., and Batina N., (2005) *Catalysis Today*, 107-108, 719-725
[18] Callejas M.A., Martinez M.T., Blasco T., Sastre W., (2001), *Applied Catalyst*, 218, 181-188.
[19] Bonardet J.L., Barrage M.C., Fraissard J., (1995) *Journal of Molecular Catalysis A: Chemical*, 96, 123-143.
[20] Barbier J., (1987) Studies in surface Science and Catalyst, Catalyst deactivation, B.Delmon and G Froment (Eds) Elsevier. Amsterdant, p.1
[21] Parera J.M., Figoli N., Traffano E., (1983), *Journal of Catalysis*, 79, 481-85
[22] van Doorn J., Barbolin H. , Moujlin J.A., (1992), *Ind Eng Chem. Res*., 31, 101-107
[23] Zuo D., Vrinat M., Nie H., Mauge F., Shi Y., Lacroix M., Li D., (2004), *Catalysis Today*, 93-95, 751-760.
[24] Gajardo P., Mathieux A, Grange P., Delmon B. , (1982), *Applied Catalyst*, 3, 347-352.
[25] Silva-Rodrigo R., Calderón-Salas C., Melo Banda J.A., Domínguez J.M. and Vázquez-Rodríguez A.,. (2004), *Catalysis Today*, *98,1-2*, *2004*, *123-129.*
[26] Galiasso Tailleur R., and Prada Silvy P.R.,"Effect of catalyst pretreatment in Mildhydrocracking operation", (2003) Preprint of Sixth Internacional Conference of Refinery section at the AICHE meeting New Orleans April, 234-25
[27] Ti Arillo M.A., Lopez M.L., Pico C., Veiga M.L., Jiménez Lopez A., Rodriguez Castillon E., (2001) *Journal of Alloys and Compounds*, 317-318, (2001), 160-163.

[28] Duchet J.C., Lavalley J.C., Housni S., Ouani D., Bachelier J., Lakhdar M., Mnnour A., Cornet D., (1988) *Catalysis Today* 4, 71-75.
[29] Zuo D., Li D., Nie H., Shi Y., Lacroix M., Vrinat M., (2004), *Journal of molecular Catalysis. A: Chem*., 211, 179-83.
[30] Cerqueira H.S., Ayrault P., Datka J., Magnoux P., Guisnet M., (2000) *Journal of Catalysis.*, 196, 149-156.
[31] Corma A., Fornes V., Navarro M.T., Perez-Pariente J., (1994) *Journal of Catalysis,* 148, 569-572.
[32] Meloni D., Martin P., Ayrault P., Guisnet M., (2001) *Catalyst Letters*; 71,3-4, 213-217.
[33] Galiasso Tailleur R.,(2005), *Computer and Chemical Engineering,* 29, 11-12, 2404-2419.
[34] Kubicka D., Kumar N., Maki-Arvela P., Tiitta M., Niemi V., Karhu H., Salmi T., Murzin D.Y.; (2004), *Journal of Catalysis*, 227, 313-327.
[35] Nylén U., Sassu L., Melis S., Järås S., Boutonnet M., (2006), *Applied Catalysis A: General*, 299, 17, 1-13
[36] Santikunaporn M., Herrera J.E., Jongpatiwut S., Resasco D.E., Alvarez W.E.,. Sughrue E., (2004), *Journal of Catalysis,* 228, 1, 100-113.
[37] McVicker G.B.,Daage L.M., Touvelle M.S., Hudson C.W., Klein D.P., Baird W.C., Cook B.R, Chen J.G., Hantzer S., Vaughan D.E.W., Ellis E.S., and Feeley O.C., (2002), *Journal of Catalysis*, 210, 137–148
[38] Arroyo J. , and Galiasso Tailleur R., "Kinetics model for n-C_{16} hydrocracking in presence of di-aromatics and DBT" (2006) submit to *Ind. Eng. Chem. Res. & Dev*
[39] Galiasso Tailleur R., (2006), *Fuel Processing Technology.* 87. 9, 759-767.
[40] Ding L., Zheng Y., Zhang Z., Ring Z. and Chen J.; (2006), *Journal of Catalysis*, 241, 2, 435-445
[41] Vriniat M.L.; (1983), *Applied Catalysis,* 6, 137-142
[42] Houlla M., Nag N.K., Sapre A.V., Broderick D.H., Gates B.C., (1978), *AICHE Journal*, 24, 1015-19.